Evidence for Coupled Electron and Proton Transfer in the [8Fe-7S] Cluster of Nitrogenase†

William N. Lanzilotta,‡ Jason Christiansen,§ Dennis R. Dean,§ and Lance C. Seefeldt*,†

Department of Chemistry and Biochemistry, Utah State University, Logan, Utah 84322, and the Department of Biochemistry and Anaerobic Microbiology, Virginia Polytechnic Institute and State University, Blacksburg, Virginia 24061

Received January 7, 1998; Revised Manuscript Received June 8, 1998

ABSTRACT: Substrate reduction by nitrogenase requires electron transfer from a [4Fe-4S] cluster in the iron (Fe) protein component to an FeMo cofactor in the molybdenum−iron (MoFe) protein component in a reaction that is coupled to MgATP hydrolysis and component protein association and dissociation. An [8Fe-7S] (or P-) cluster in the MoFe protein has been proposed as an intermediate electron-transfer site, although how this cluster functions in electron-transfer remains unclear. In the present work, it is demonstrated that one redox couple of the P-cluster ($P^{2+/1+}$) undergoes coupled electron and proton transfer, whereas a more reduced couple ($P^{1+/N}$) does not involve a coupled proton transfer. Redox titrations of the MoFe protein P-cluster were performed, and the midpoint potential of the $P^{2+/1+}$ couple (E_{m2}) was found to be pH dependent, ranging from −224 mV at pH 6.0 to −348 mV at pH 8.5. A plot of E_{m2} versus the pH for this redox couple was linear and revealed a change of −53 mV/pH unit, indicating a single protonation event associated with reduction. From this plot, it was concluded that pK_a^{P2+} is <6.0 and pK_a^{P1+} is >8.5 in a proton-modified Nernst equation. In contrast, the midpoint potential for the $P^{1+/N}$ couple (E_{m1}) was found to be −290 mV and was invariant over the pH range 6.0−8.5. These results indicate that the protonated species does not influence either the P^{1+} or the P^N oxidation states. In addition, at physiological pH values, electron transfer is coupled to proton transfer for the $P^{2+/1+}$ couple. The P-clusters are unique among [Fe-S] clusters in that they appear to be ligated to the protein through a serinate-γO ligand (βSer188) and a peptide bond amide-N ligand (αCys88), in addition to cysteinate-S ligands. Elimination of the serinate ligand by replacement with a glycine was found to shift the E_m values for both P-cluster couples by greater than +60 mV, however the pH dependence of E_{m2} was unchanged. These results rule out Ser188 as the protonated ligand responsible for the pH dependence of E_{m2}. The implications of these results in understanding the nitrogenase electron-transfer mechanism are discussed.

The reduction of substrates by nitrogenase requires electron transfer from the [4Fe-4S] cluster of the iron (Fe) protein component ultimately to the [7Fe−Mo-9S-homocitrate] cofactor (FeMoco) in the molybdenum−iron (MoFe) protein component, the site of substrate reduction (*1*−*4*). The transfer of each electron between the component proteins is coupled by an unknown mechanism to the hydrolysis of a minimum of two MgATP molecules bound to the Fe protein component (*1*−*3*, *5*). Following each single electron-transfer event, the oxidized Fe protein, with two bound MgADP molecules, is believed to dissociate from the one-electron-reduced MoFe protein (*6*). The Fe protein is reduced, and the MgADP molecules are exchanged for MgATP molecules. This cycle is repeated until sufficient electrons have accumulated within the MoFe protein to reduce the bound substrate. Nitrogenase can reduce a range of substrates by multiples of two electrons (*1*, *7*, *8*). While little is known about the details of substrate binding or reduction by nitrogenase, it is clear that all substrate reduction reactions catalyzed by nitrogenase involve multiples of two electrons and are coupled to proton transfer (*9*). The Fe protein is the only known electron donor to the MoFe protein that will support substrate reduction. Among questions remaining

† This work was supported by National Science Foundation Grants MCB-9722937 to L.C.S. and MCB-9630127 to D.R.D. and by a United States Department of Agriculture Postdoctoral Fellowship (USDA-9603167) to J.C.

* Address correspondence to this author. Phone (435) 797-3964. Fax: (435) 797−3390. E-mail: seefeldt@cc.usu.edu.

‡ Utah State University.

§ Virginia Polytechnic Institute and State University.

[1] Abbreviations: Fe protein, iron protein of nitrogenase; MoFe protein, molybdenum−iron protein of nitrogenase; MES, 2-[4-morpholino]ethanesulfonic acid; MOPS 3-[*N*-morpholino]propanesulfonic acid; Tricine, *N*-[tris-(hydroxymethyl)methyl] glycine; CHES, 2-[*N*-cyclohexylamino]ethanesulfonic acid; E_m, midpoint potential; E°_A, standard reduction potential for the deprotonated cluster couple; E°_{AH}, standard reduction potential for the protonated cluster couple; E_{m1}, midpoint potential for the $P^{1+/N}$ couple, E_{m2}, midpoint potential for the $P^{2+/1+}$ couple; P-cluster, [8Fe-7S] cluster of the MoFe protein; P^N, oxidation state of the P-cluster with all iron atoms ferrous; P^{1+}, P-cluster one-electron oxidized from the P^N state; P^{2+}, P cluster two-electron oxidized from the P^N state; M center, iron−molybdenum cofactor of nitrogenase; K_a^{P2+}, proton equilibrium constant for the P^{2+} state; K_a^{P1+}, proton equilibrium constant for the P^{1+} state; K_a^{PN}, proton equilibrium constant for the P^N state; IDS, indigo disulfonate.

S0006-2960(98)00048-8 CCC: $15.00
Published on Web 07/23/1998

about the nitrogenase mechanism are how electrons are accumulated within the MoFe protein and how electrons are delivered to FeMoco.

Each MoFe protein tetramer contains two additional metal clusters, [8Fe-7S] clusters (also called the P-clusters), that have been implicated as possible electron-transfer intermediates between the Fe protein and FeMoco (*10*−*13*). This suggestion has evolved from several observations. The MoFe protein is an $\alpha_2\beta_2$ tetramer, with each $\alpha\beta$-dimer apparently functioning as an independent catalytic unit. Each $\alpha\beta$-dimer unit contains one active-site FeMoco located within the α-subunit, and one P-cluster bridged between the $\alpha\beta$-subunits (*14*). Recent X-ray crystal structures of two stable Fe protein−MoFe protein complexes place the P-clusters near the Fe protein−MoFe protein docking interface (*15*, *16*). This places each P-cluster between the Fe protein [4Fe-4S] cluster and the MoFe protein FeMoco and suggests that each P-cluster might participate as an electron-transfer intermediate between the Fe protein and the FeMoco. In addition to this structural evidence, studies with altered MoFe and Fe proteins also suggest that the P-clusters can act as initial electron acceptors from the Fe protein. In one study, a catalytically inactive form of the MoFe protein was created by substitution of FeMoco with an acid treated and modified FeMoco derivative (*13*). The MoFe protein with this modified FeMoco was inactive in substrate reduction, but was found to accept electrons from the Fe protein. Following electron transfer from the Fe protein, an increase in the intensity of an EPR signal assigned to the P-clusters was observed. This $g = 2$ region EPR signal integrated to one spin per P-cluster, suggesting that the electron transferred from the Fe protein went to the P-cluster (*13*). In a separate study, amino acids within the MoFe protein located between the P-clusters and the FeMoco were substituted to test the possible role of these residues in electron transfer from the P-clusters to FeMoco (*10*). Stopped-flow spectroscopic results indicated that electrons transferred from the Fe protein accumulated on the P-clusters before proceeding to FeMoco. It was proposed that an electron-transfer pathway from the P-clusters to FeMoco had been disrupted and that the P-clusters were accumulating electrons transferred from the Fe protein. Stopped-flow and EPR spectroscopic results obtained during the reduction of dinitrogen revealed that the P-clusters were oxidized following the four electron reduction of bound nitrogen (*12*). It was suggested that the P-clusters transferred electrons to FeMoco required for the reduction of bound N_2 (*12*).

The P-clusters of nitrogenase are so far unique among biological [Fe-S] clusters in several ways (*17*). First, the overall structure is of two bridged cubane [4Fe-4S] subclusters with a common bridging μ6-sulfide at one corner (*18*). [Fe-S] clusters often function in one-electron-transfer reactions (*17*), and thus the unique structure of the P-cluster offers the possibility of delivering two electrons. Second, the P-clusters are the only known case of an [Fe-S] cluster that naturally contains serinate O and amide N ligands as well as the usual cysteinate S ligands. Recent X-ray crystallographic studies of two oxidation states of the MoFe protein have revealed that the P-clusters undergo structural rearrangements upon oxidation or reduction, one consequence of which is the displacement of both the serinate O and amide N ligands from the P-cluster upon reduction (*18*). Other proteins that contain stable [Fe-S] clusters with cysteinate S or aspartate O ligation have been modified by site-directed mutagenesis to replace one or more of the ligands with serinate O ligands (*19*−*31*). Interestingly, at least two of these [Fe-S] clusters having serinate ligation exhibit a pH-dependent midpoint potential (E_m) (M. K. Johnson, personal communication; A. G. Wedd, personal communication). It has been suggested that such pH dependence is the result of proton transfer to the alkoxide O atom of the cluster serinate ligand.

In light of the novel serinate O and amide N ligation of the P-cluster and the recent evidence for the displacement of these ligands upon reduction of the P-cluster, it seemed possible that these ligands might be involved in protonation reactions, thus rendering the E_m for one or more of the redox couples pH dependent. In the present work, the pH dependence of the E_m values for two of the P-cluster redox couples was examined. Also, site-directed mutagenesis was employed to investigate the possible involvement of the serinate ligand at position 188 of the MoFe protein β-subunit in the coupled electron and proton-transfer reactions proposed here.

EXPERIMENTAL PROCEDURES

MoFe Proteins. Wild-type nitrogenase MoFe protein was expressed in *Azotobacter vinelandii* cells grown under N_2-fixing conditions (*32*). Mutagenesis of the *A. vinelandii nifK* gene encoding the β-subunit of the MoFe protein was performed as previously described (*33*). For construction of mutant strain DJ1017, which has the MoFe protein β-subunit serine 188 residue substituted by glycine 188, an AGC codon was substituted by a GGC codon. Although this mutant is capable of diazotrophic growth, it grows at a rate substantially lower (4.3 h doubling time) than the wild-type strain (2.1 h doubling time). Both the wild-type and β-Ser188Gly-modified MoFe proteins were purified essentially as previously described (*32*), except that all buffers used in the purification of the β-Ser188Gly MoFe protein contained 20% (v/v) glycerol, and the heat step was eliminated. The purified MoFe proteins were homogeneous as determined by coomassie blue staining of a sodium dodecyl sulfate−polyacrylamide gel (*34*). Protein concentrations were determined by a modified biuret method (*35*) and from the visible absorption using an absorption coefficient of 62.3 mM^{-1} cm^{-1} at 400 nm (*36*). The wild-type MoFe protein used had a specific activity greater than 2300 nmol of H_2 produced min^{-1} mg^{-1} (*37*). The altered MoFe protein (β-S188G) had a specific activity of 1490 nmol of H_2 produced min^{-1} mg^{-1}. The reduced activity exhibited by the altered MoFe protein is in line with the lower growth rate when cultured under diazotrophic conditions when compared to the wild-type strain. All protein manipulations were performed in an argon-filled glovebox (Vacuum Atmospheres Co., Hawthorne CA).

Redox Titrations of Wild-Type and β-Ser188Gly MoFe Proteins. Potentiometric redox titrations were performed

[2] The formal charges of the [8Fe-7S] cluster core corresponding to the P^{2+}, P^{1+}, and P^N oxidation states would be 4+, 3+, and 2+, respectively.

essentially as previously described (*38*, *39*). For titrations of the wild-type MoFe protein, the buffer contained 250 mM NaCl and 25 mM each of MES (pK_a = 6.1), MOPS (pK_a = 7.2), Tricine (pK_a = 8.1), and CHES (pK_a = 9.3). Redox titrations of the β-S188G MoFe protein were performed in a buffer solution consisting of 50 mM each of MOPS and Tricine and 250 mM NaCl. In separate experiments, it was confirmed that the choice of buffers did not alter the intensity of the EPR signals nor the determined E_m values for either MoFe protein sample. MoFe protein samples were prepared for redox titrations by passage through a Sephadex G-25 column equilibrated with the indicated buffer adjusted to the specified pH value. For all redox titrations in the −100 to −500 mV potential range, the redox mediators indigo disulfonate (IDS) (E_m = −125 mV), flavin mononucleotide (E_m = −172 and −238 mV), benzyl viologen (E_m = −361 mV), and methyl viologen (E_m = −440 mV) were added to final concentrations of 100 μM each (38). For redox titrations above −100 mV, the mediators methylene blue (E_m = +11 mV) and 2,6-dichlorophenol-indophenol (E_m = +220) were also included at final concentrations of 100 μM. While the E_m value for some of the mediators is pH dependent, this was not a problem since the potential of the bulk solution was always measured. The redox potential of the titration solution was adjusted by the addition of aliquots of a 5 mM dithionite ($Na_2S_2O_4$) solution, a 5 mM oxidized indigo disulfonate solution, or a 5 mM oxidized methylene blue solution. When the desired potential was reached, the solution was allowed to stir for 10 additional min to reach equilibrium, and then a 250 μL aliquot was removed from the titration solution and was immediately frozen in a calibrated quartz EPR tube (Wilmad Co., Buena, NJ). Measurement of the pH of the solution at the end of a titration confirmed that the pH had not changed significantly. The final concentration of the MoFe protein ranged 50−100 μM. The reference electrode was a Ag/AgCl microelectrode that was calibrated against a standard calomel electrode (*38*). All potentials are reported relative to the normal hydrogen electrode (NHE).

Analysis of Titration Data. The relative concentration of the P^{2+} state of the P-cluster was quantified from the intensity of the $S \geq 3$ parallel mode EPR signal at g = 11.8 (*11*, *38*). The relative concentration of the P^{1+} state of the P-cluster was quantified from the intensity of the $S = {}^1/_2$ perpendicular mode EPR signal at g = 2.05, 1.94, and 1.81 (*40*). The EPR signals arising from the $S = {}^5/_2$ spin state of the P^{1+} oxidation state were also monitored and showed similar behavior to the $S = {}^1/_2$ signals, ruling out a spin-state conversion between the ${}^5/_2$ and ${}^1/_2$ spin states. In each case, the signal intensity was determined from the peak to peak height or from the peak to baseline height and was corrected for the protein concentration. Given the broadness of these signals, it was found that signal peak height was a better monitor of oxidation state than the integrated area under the peaks. For the P^{2+} ($S \geq 3$) EPR signal, relative signal intensities were determined by comparing each signal intensity to the maximum intensity observed at positive potentials. For the P^{1+} ($S = {}^1/_2$) EPR signal, relative signal intensities were determined by comparing each signal intensity to the maximum signal intensity observed at −225 mV and pH 6.5. The relative signal intensities for both the P^{1+} and P^{2+} EPR signals were plotted against the applied potential, and each data set was fit to the Nernst equation (eq 1)

Scheme 1

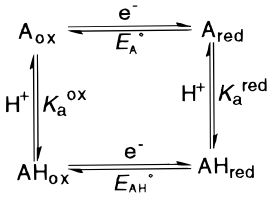

$$E = E_m + \frac{59}{n}\log K \quad (1)$$

where the temperature was 25 °C, E_m is the midpoint potential, E is the applied potential, n is the number of electrons involved in the redox reaction, and K is the equilibrium constant of [oxidized]/[reduced].

A coupled electron and proton-transfer reaction can be depicted by Scheme 1 where A_{ox} is the oxidized, unprotonated state, AH_{ox} is the oxidized, protonated state, A_{red} is the reduced state, and AH_{red} is the reduced, protonated state. K_a^{ox} and K_a^{red} are the equilibrium constants for proton transfer to the oxidized or reduced states, respectively, and E°_{AH} and E°_A are the standard reduction potentials for the protonated and deprotonated couples, respectively. For such a reaction scheme, eqs 2 and 3 can be derived at 298 K

$$E_m = E^\circ_A + 59 \log \frac{K_a^{ox}(K_a^{red} + [H^+])}{K_a^{red}(K_a^{ox} + [H^+])} \quad (2)$$

$$E_m = E^\circ_{AH} + 59 \log \frac{(K_a^{red} + [H^+])}{(K_a^{ox} + [H^+])} \quad (3)$$

where all of the parameters have the meaning described earlier (*41*).

The E_m values measured at each pH were plotted against the pH providing estimates of E°_A, E°_{AH}, K_a^{red} and K_a^{ox}. Nonlinear and linear least-squares fits were performed using the computer program Igor Pro (Wavemetrics, Lake Oswego, OR).

EPR Spectroscopy. EPR spectra were recorded on a Bruker ESP300E spectrometer equipped with a dual mode cavity and an Oxford ESR 900 liquid helium cryostat. EPR spectra acquired in parallel mode were recorded at 12 K with a microwave power of 6.36 mW, a microwave frequency of 9.39 GHz, a modulation amplitude of 7.102 G, a modulation frequency of 100 kHz, a time constant of 10.24 ms, and a conversion time of 10.24 ms. In each case, the final spectrum was the sum of 20 scans. EPR spectra acquired in perpendicular mode were recorded at 12 K with a microwave power of 2.01 mW, a microwave frequency of 9.64 GHz, a modulation amplitude of 5.028 G, a modulation frequency of 100 kHz, a time constant of 10.24 ms, and a conversion time of 10.24 ms. In each case, the final spectrum was the sum of 10 scans.

RESULTS

EPR Spectra of the P^{1+} and P^{2+} States of the P-Cluster. The nitrogenase MoFe protein is normally purified in the

Scheme 2

$$P^{N} \underset{e^-}{\overset{E_{m1} = -309\ mV}{\rightleftharpoons}} P^{1+} \underset{e^-}{\overset{E_{m2} = -309\ mV}{\rightleftharpoons}} P^{2+} \underset{e^-}{\overset{E_{m3} = +90\ mV}{\rightleftharpoons}} P^{3+} \longrightarrow P^{superox}$$

presence of the reductant dithionite ($S_2O_4^{2-}$), which serves as an oxygen scavenger to protect the MoFe protein from O_2 inactivation and maintains the MoFe protein in a reduced state. In this state, the MoFe protein is active and is known to accept electrons from the Fe protein. In the presence of dithionite, the P-clusters are in a reduced state that has been designated as P^N. Mossbauer spectroscopy indicates that, in this state, all eight iron atoms are in the ferrous (+2) oxidation state resulting in an $S = 0$ spin system that is EPR silent (*42*). One of the intriguing questions about the P-clusters is how an [Fe-S] cluster with all of the irons in the ferrous oxidation state can accept electrons. There is currently no evidence that the P-clusters can be reduced beyond the P^N state (*1*). Given the probable limitation to further reduction and the circumstantial evidence that oxidized states of the P-cluster may be involved in electron transfer during nitrogenase turnover (*11*, *12*), understanding the properties of the oxidized states of the P-cluster is of interest as an approach toward understanding the electron-transfer mechanism in nitrogenase.

The P-clusters of the MoFe protein have been prepared in at least five different stable oxidation states as summarized in Scheme 2 (*40*, *43*). Starting at the reduced P^N state, the P-cluster can be reversibly oxidized by up to three electron equivalents to oxidation states designated P^{1+}, P^{2+}, and P^{3+}, each one electron oxidized relative to the previous state (Scheme 2). Further oxidation of the P-clusters beyond the P^{3+} oxidation state is irreversible (*43*), and thus, these "superoxidized" states are probably not relevant to the nitrogenase mechanism. Both the P^{1+} and P^{2+} states are paramagnetic. The P^{1+} state has a mixed spin system ($S = {}^1/_2$ and ${}^5/_2$) with perpendicular mode EPR signals in the $g =$ 2 and 5 regions (*40*), and the P^{2+} state has an integer spin system ($S \geq 3$) with a parallel-mode EPR signal at $g = 11.8$ (*43*). The P^{3+} state is an $S = {}^1/_2$ and ${}^7/_2$ mixed spin system. The midpoint potentials (E_{m1}, E_{m2}, and E_{m3}) for the three reversible P-cluster couples (Scheme 2) have been determined at pH 8.0 to be −309, −309, and +90 mV, respectively (*43*). In these studies, an EPR signal for the P^{1+} oxidation state was not observed, but values for E_{m1} and E_{m2} were inferred from the two electron redox reaction.

The first indication that one or more of the P-cluster E_m values might be pH dependent came from the observation that the P^{1+} EPR signal could be observed if the pH of the titration was lowered from 8.0 to 7.4 (*40*). An explanation for this observation was not provided at the time, but one possibility is that one or more of the E_m values is pH dependent, and in lowering the pH, it is possible to populate the P^{1+} state.

To explore the possible pH dependence of the P-cluster redox couples, the MoFe protein was poised at different applied potentials at different pH values (8.0 or 6.5), and the intensities of the P^{2+} and P^{1+} EPR signals were monitored. Figure 1 illustrates representative EPR spectra observed for both the P^{2+} (panel A) and the $S = {}^1/_2$ spin state of the P^{1+} (panel B) oxidation states at two different pH values. The maximum intensity for the P^{2+} EPR signal

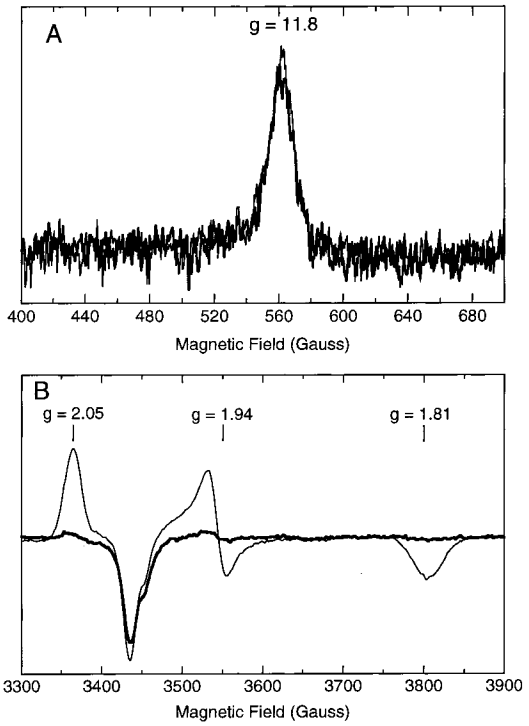

FIGURE 1: pH dependence of the EPR signals for the P^{2+} ($S \geq 3$) and P^{1+} ($S = {}^1/_2$) oxidation states of the P-cluster. Reductive titrations of the P^{2+} oxidation state of the MoFe protein (92 μM) were performed as described in the Experimental Procedures. (Panel A) Parallel mode EPR spectra of the P^{2+} state of the MoFe protein are shown at pH 8.0 and at a potential of −180 mV (thick line) and at pH 6.5 and at a potential of −130 mV (thin line). (Panel B) Perpendicular mode EPR spectra of the P^{1+} state of the MoFe protein are shown at pH 8.0 and at a potential of −307 mV (thick line), and at pH 6.5 and at a potential of −267 mV (thin line). EPR conditions are described in the Experimental Procedures. Potentials are relative to the normal hydrogen electrode (NHE).

was observed at either pH 8.0 or pH 6.5 when similar potentials were applied. In contrast, the intensity of the P^{1+} EPR signal was dramatically different at pH 8.0 when compared to pH 6.5. One way to explain these results is that there is a pH dependence of one or both of the E_m values (E_{m1} or E_{m2}), resulting in a significant increase in the equilibrium concentration of the P^{1+} oxidation state at lower pH values.

pH Dependence of the P-Cluster Redox Couples. To investigate the pH dependence of the P-cluster redox couples, redox titrations monitoring the P^{2+} and P^{1+} EPR signals of the P-cluster were performed at a number of pH values. Figure 2 illustrates the intensity of the EPR signal for the P^{2+} oxidation state as a function of applied potential at different pH values. E_{m2} was found to be dependent on pH, shifting to more positive potentials at lower pH values. The value of E_{m2} ranged from −224 mV at pH 6.0 to −348 mV at pH 8.5. By monitoring the EPR signal of the P^{1+} oxidation state, it is possible to establish the E_m values both for the $P^{1+/N}$ couple (at more negative potentials) and for the $P^{2+/1+}$ couple (at more positive potentials). Figure 3 illustrates the intensity of the EPR signal for the P^{1+} state as a function of applied potential at different pH values. The interconversion

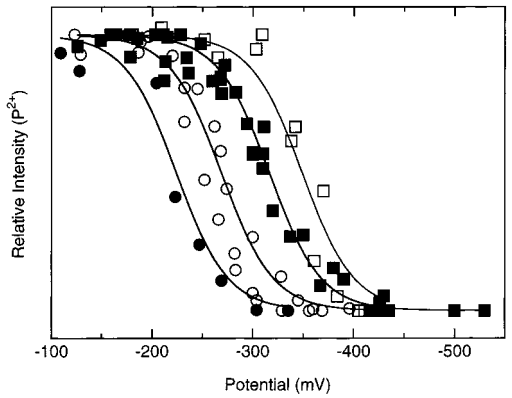

FIGURE 2: Redox titrations of the P^{2+} oxidation state of the P-clusters at different pH values. Redox titrations of the P^{2+} oxidation state of the MoFe protein (92 μM) at different pH values were performed as described under Experimental Procedures. The relative intensity of the parallel mode EPR signal of the P^{2+} ($S \geq 3$) state is plotted against the solution potential at pH 6.0 (●), pH 7.0 (○), pH 8.0 (■), and pH 8.5 (□). The solid lines represent nonlinear least-squares fits of the data to the Nernst equation (eq 1) where $n = 1$, and the calculated redox potentials were found to be −224, −270, −320, and −348 mV, respectively.

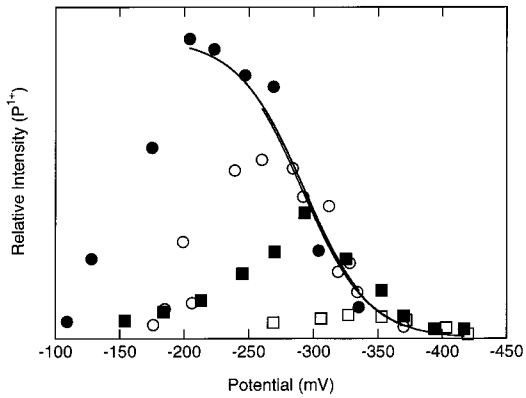

FIGURE 3: Redox titrations of the P-clusters monitoring the P^{1+} oxidation state at different pH values. Reductive titrations of the MoFe protein (92 μM) starting with the P^{2+} oxidation state at different pH values were performed as described in the Experimental Procedures. The relative intensity of the perpendicular mode EPR signal of the P^{1+} ($S = {}^1/_2$) state is plotted against the solution potential at pH 6.0 (●), pH 6.5 (○), pH 7.0 (■), and pH 7.5 (□). The development of the P^{1+} EPR signal is apparent from the data at more positive potentials. The subsequent decrease in the P^{1+} EPR signal was fit to the Nernst equation with $n = 1$ (downward sloping solid lines at more negative potentials). The maximum intensity for the P^{1+} state EPR signal was taken to be the value determined at pH 6.0 and −200 mV.

between the P^N and P^{1+} states (right side of the figure) was independent of pH and gave an E_{m1} of −290 mV. In contrast, the interconversion between the P^{2+} and P^{1+} oxidation states (left side of the figure) was dependent on the pH, with more positive E_{m2} values at lower pH values. The EPR signal for the $S = {}^5/_2$ spin state of P^{1+} was also monitored by EPR and was found to coincide with the intensity of the $S = {}^1/_2$ spin state EPR signal, ruling out a spin state conversion. This result is consistent with the pH dependence of E_{m2} found from the experiments shown in Figure 2. Thus, E_{m2} is pH dependent while E_{m1} is not. It is also apparent from Figure 3 that the P^{1+} state and its EPR signal can be maximized at lower pH values compared to higher pH values.

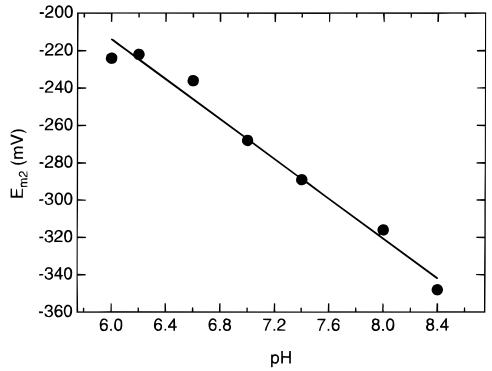

FIGURE 4: pH dependence of the midpoint potential for the $P^{2+/1+}$ couple of the P-cluster. The midpoint potentials (E_{m2}) for the $P^{2+/1+}$ couple at different pH values were determined as described in the legend to Figure 2 and were plotted against the pH value. Fit of the data to a straight-line revealed a slope of −53 mV/pH unit.

To quantify the pH dependence of E_{m2}, the measured E_{m2} values were plotted against pH value (Figure 4) where E_{m2} = −224 mV at pH 6.0, −222 mV at pH 6.2, −240 mV at pH 6.5, −270 mV at pH 7.0, −290 mV at pH 7.5, −320 mV at pH 8.0, and −348 mV at pH 8.5. Over the pH range from 6.0 to 8.5, E_{m2} versus pH data were nearly linear, having a slope of −53 mV/pH unit. When the point at pH 6.0 was not included, the slope was −59 mV/pH unit, identical to the theoretical value for the coupling of a single proton transfer with each electron transfer. For the $P^{2+/1+}$ couple, redox cycling at pH values between 6.0 and 8.5 requires that electron transfer is coupled to proton transfer. These reactions can be described by the general relationships shown in Scheme 1, where there are two pK_a values, one for the protonation reactions of the reduced (P^{1+}) state (pK_a^{P1+}) and one for the protonation reactions of the oxidized (P^{2+}) state (pK_a^{P2+}). There are also two E_m values, one for the fully protonated species (E°_{Hm2}) and one for the fully unprotonated species (E°_{m2}). Because the E_m versus pH data for the $P^{2+/1+}$ couple is approximately linear over the pH range examined, it is not possible to establish exact values for any of these four parameters. However, estimates for the parameters of the proton modified Nernst equation (eqns 2 and 3) were found to be $pK_a^{P2+} < 6.0$, $pK_a^{P1+} > 8.5$, (E°_{Hm2}) > −224 mV, and (E°_{m2}) < −348 mV. An important consequence of the two pK_a values for this couple of the P-cluster is that at any pH value between 6.0 and 8.5, it is predicted that each electron-transfer event will be coupled to a proton-transfer event.

Effects of Fe Protein−MoFe Protein Complex Formation on the P-Cluster Couples. Upon binding of the Fe protein to the MoFe protein, there are marked changes in the E_m values for both the Fe protein [4Fe-4S] cluster redox couple (2+/1+) and the MoFe protein P-cluster $P^{ox/N}$ redox couples (*38*). These experiments made use of a nondissociating Fe protein−MoFe protein complex formed by an altered Fe protein (L127Δ) (*44*). To determine if Fe protein−MoFe protein complex formation alters the pH dependence of the P-cluster couples, the L127Δ Fe protein−MoFe protein tight complex was formed, and the E_{m1} and E_{m2} values were established at different pH values. It was found that the binding of the Fe protein to the MoFe protein did change the E_m values for the P-cluster couples to more negative values (as previously shown) (*38*), but had no impact on the

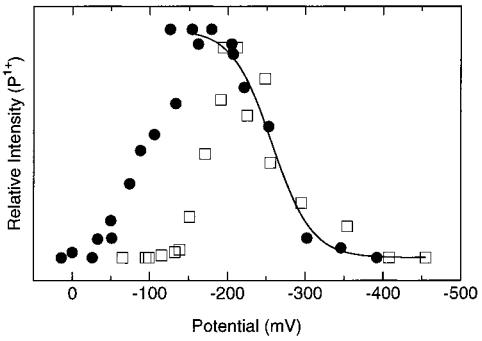

FIGURE 5: Redox titrations of the P^{1+} oxidation state of the P-clusters at different pH values for the β-Ser188Gly altered MoFe protein. Oxidative titrations starting from the P^N state of the P-clusters for the β-Ser188Gly altered MoFe protein (80 μM) were performed as described in the Experimental Procedures. The relative intensity of the perpendicular mode EPR signal of the P^{1+} ($S = {}^1/_2$) state is plotted against the solution potential at pH 7.0 (●) and pH 8.0 (□). The solid lines represent nonlinear least-squares fits of the data to the Nernst equation where $n = 1$. The calculated redox potentials for the $P^{1+/N}$ couple were −260 mV at both pH values and for the $P^{2+/1+}$ couple were −174 mV at pH 8.0 and −90 mV at pH 7.0.

pH dependence of E_{m2} or the lack of a pH dependence of E_{m1}.

β-Ser188Gly Altered MoFe Protein. The pH dependence for E_{m2}, but not for E_{m1}, indicates that the protonatable species only influences the P^{2+} state. The noncysteinate ligands to the P-cluster (βSer188-γO and αCys88-amide N) are both obvious candidates for the site of protonation because both ligands are predicted to be protonatable and are known to be displaced from the P-cluster upon reduction (*18*). The finding from the current work of a single protonation reaction for the $P^{2+/1+}$ couple is somewhat surprising given the prediction that both the serinate and amide ligands might be protonated.

To test if the serinate ligand is responsible for the pH dependence of E_{m2}, this residue was substituted with a glycine residue by means of site-directed mutagenesis and gene replacement. This substitution eliminates the possible alkoxide ligand. The β-Ser188Gly-altered MoFe protein was stable and could be purified in quantities comparable to the wild-type MoFe protein. The EPR spectrum of the β-Ser188Gly altered MoFe protein in the presence of the reductant dithionite was nearly identical to that observed for the wild-type MoFe protein. In this state, the $S = {}^3/_2$ spin state of the FeMoco gives rise to EPR inflections at $g =$ 4.30, 3.65, and 2.00. With the wild-type MoFe protein, treatment with a slight excess of the oxidized mediator indigo disulfonate (IDS) ($E_m = -125$ mV) results in the oxidation of the P-clusters to the P^{2+} oxidation state (*43*). The E_m for the first oxidized couple of FeMoco ($M^{ox/N}$) is −41 mV (*43*) and, thus, is not accessed by IDS. Treatment of the β-Ser188Gly-altered MoFe protein with oxidized IDS did not result in the formation of the P^{2+}-state EPR signal, suggesting that either the E_m values for the two couples had been shifted or the $S \geq 3$ spin system had been perturbed by the absence of the serinate ligand. It was found that treatment of the β-Ser188Gly-altered MoFe protein with the oxidized mediator methylene blue ($E_m = +11$ mV) resulted in the formation of the P^{1+} EPR signal, indicating that one or both of the E_m values for the two couples had been shifted to more positive potentials. A redox titration of the

Scheme 3

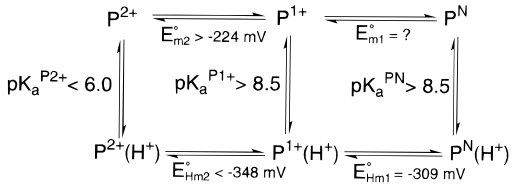

β-Ser188Gly-altered MoFe protein was performed at two different pH values (7.0 and 8.0), and the concentration of the P^{1+} oxidation state was monitored by EPR signal intensity. As mentioned earlier, the E_m values for both the $P^{2+/1+}$ and the $P^{1+/N}$ oxidation states can be monitored from the appearance and subsequent disappearance of the P^{1+} state EPR signal during oxidative titrations. Figure 5 illustrates such an oxidative titration for the β-Ser188Gly-altered MoFe protein. The E_{m1} for the $P^{1+/N}$ couple (right side of Figure 5) did not vary with pH and had a value of −260 mV. Thus, removal of the β-Ser188 ligand does not alter the lack of a pH dependence of E_{m1}, but does shift the E_{m1} by + 50 mV. E_{m2} can be found from the disappearance of the P^{1+} EPR signal upon oxidation (left side of Figure 5). In this case, E_{m2} remains pH dependent, with more positive potentials observed at lower pH values. It is also apparent that, at a given pH value, E_{m2} shifts approximately +136 mV. It is interesting that an EPR signal corresponding to the P^{2+} state was never observed for the β-Ser188Gly-altered MoFe protein, suggesting that removal of the serinate ligand changes the electronic properties of the P^{2+} oxidation state. The reversibility of the redox reactions for the β-Ser188Gly MoFe protein was confirmed by rereduction of the P^{2+} oxidation state back to the P^N state. In addition, it was confirmed that greater than 90% of the catalytic activity of the β-Ser188Gly MoFe protein was retained even after holding the protein for 1 h at + 11 mV. Likewise, the β-Ser188Gly MoFe protein was found to contain approximately the same number of total Fe atoms as the wild-type MoFe protein even after redox cycling. Thus, it can be concluded that redox reactions for the β-Ser188Gly MoFe protein between the P^N and P^{2+} state are reversible.

DISCUSSION

The results presented in this work provide new insights into the properties of the unique P-clusters of nitrogenase, and suggest possible roles for the coupling of proton and electron-transfer reactions in these clusters to the nitrogenase substrate reduction mechanism.

Coupled Proton and Electron Transfer in the Nitrogenase P-Clusters. The properties of the P-clusters deduced from the present studies can be summarized by the reactions illustrated in Scheme 3. In this model, electron-transfer reactions are shown left to right and proton-transfer reactions are shown top to bottom. One of the significant findings of the present work is that E_{m2} for the $P^{2+/1+}$ couple is pH dependent. This redox couple of the P-cluster is best described by the four-state model shown on the left side of Scheme 3 and the four parameters E_{m2}, E_{Hm2}, pK_a^{P2+}, and pK_a^{P1+} in the modifed Nernst equations (eqs 2 and 3). Estimates for these four parameters of $E_{m2} < -348$ mV, $E_{Hm2} < -224$ mV, $pK_a^{P2+} < 6.0$, and $pK_a^{P1+} > 8.5$ were

obtained. Thus, as the pH is lowered, E_{m2} becomes more positive, with a predicted range from −224 to −348 mV. Near physiological pH values (approximately 7.0), the P^{2+} state is expected to exist predominately (>99%) in the unprotonated state (top left corner of Scheme 3). Upon reduction to the P^{1+} state, a proton transfer must occur, resulting in predominately (>99%) the protonated state [$P^{1+}(H^+)$]. A prediction of the current model is that electron- and proton-transfer reactions will be linked for this redox couple near physiological pH values. This prediction is similar to models of gated proton and electron transfer that have been seen for [Fe-S] clusters in other proteins (*45*).

The lack of a pH dependence of E_{m1} for the $P^{1+/N}$ couple provides some additional insights. First, it is clear that the protonated species responsible for the pH dependence of E_{m2} does not influence the P^{1+} or P^N states. Assuming that K_a^{PN} (not measured) is similar to or larger than K_a^{P1+}, then a further prediction of the current model is that the P^N state will also exist predominately (>99%) in the protonated P^N state [$P^N(H^+)$] near physiological pH. Thus, redox reactions of the P-cluster at neutral pH values are expected to involve predominately the unprotonated P^{2+} state, the protonated $P^{1+}(H^+)$ state, and the protonated $P^N(H^+)$ state.

This model helps to explain some of the earlier confusion about the P-cluster redox reactions. For example, the apparent equivalency of the two E_m values (E_{m1} and E_{m2}) is now seen to be a special case where the pH (near 8.0) is poised at a value allowing E_{m2} to be similar to E_{m1}. At all other pH values, E_{m2} will change, becoming unequal to E_{m1}. This has important consequences in understanding the relative concentration of each of the P-cluster oxidation states at a given potential. As the pH is lowered below 8.0, E_{m2} will become more positive than E_{m1}, favoring the population of the P^{1+} oxidation state during a redox titration. For example, if the pH is 7.0, E_{m2} will be approximately −260 mV, while E_{m1} will be −310 mV. The result being that a one electron equivalent reduction of the P^{2+} state would result in predominately the P^{1+} state compared to the P^{2+} or P^N states. In contrast, at higher pH values, E_{m2} will become more negative than E_{m1}, predicting a negligible concentration of P^{1+} observed during a redox titration. Thus, it is predicted that maximal concentrations of the P^{1+} state can only be achieved at pH values below 7.0, consistent with the trend observed in earlier EPR studies (*11*, *40*).

The Protonatable Group. What then is the group that is protonated in the $P^{2+/1+}$ redox reaction? The P-clusters are not alone among [Fe-S] clusters in having a pH dependence of E_m values. In these other cases, the pH dependence of E_m has been attributed to protonation of cluster ligands, protonation of amino acids near the cluster, and protonation of one of the inorganic sulfides of the [Fe-S] cluster. All three models provide a possible explanation for the pH dependence of the $P^{2+/1+}$ couple observed in the present work.

There are several examples where a ligand to an [Fe-S] cluster is the probable site of protonation, rendering the E_m for the cluster pH dependent. For example, in Reiske [Fe-S] proteins, the [2Fe-2S] cluster is bound to the protein through two cysteinate ligands and two histidinate ligands (*46*, *47*). The E_m values for some of these proteins have been demonstrated to be pH dependent, with pK_a values for the oxidized form of the cluster that range 6.2−7.5 and pK_a values for the reduced form of the cluster that range 8.5−9.2 (*45*, *48*−*50*). It has been proposed that the histidinate ligands are the site of protonation, although this has not been shown unequivocally. While the P-clusters of nitrogenase are the only known naturally occurring case of [Fe-S] clusters bound to proteins by serinate-γO ligands, there are now several examples in which serinate ligation of an [Fe-S] cluster was created by amino acid replacement using site-directed mutagenesis. The [4Fe-4S] cluster of a ferredoxin isolated from *Pyrococcus furiosus* contains three cysteinate ligands and one aspartate ligand (*51*). Replacement of the aspartate residue with a serine residue resulted in the assembly of a [4Fe-4S] cluster, presumably with a serinate-γO ligand (*31*). This altered ferredoxin (D14S) was found to demonstrate a pH dependence of the E_m for the cluster (M. K. Johnson, personal communication). pK_a values for the oxidized and reduced states of the cluster were estimated to be <3.0 and 4.75, respectively. For this case, a model was proposed in which the alkoxide O of the serinate ligand is protonated and deprotonated. In a separate study, cysteinate ligands to the mononuclear Fe site of the *Clostridium pasteurianum* rubredoxin have been substituted with serinate ligands by means of site-directed mutagenesis. It was found that substitution of some of the cysteinate ligands by serinate ligands resulted in a pH dependence of the E_m for the redox couple (A. G. Wedd, personal communication). pK_a values for the reduced state were found to range 7.0−9.0. Proton NMR, X-ray absorption, and crystallographic studies were used to assign the alkoxide O of the serinate ligand as the protonatable species.

The recent results with serinate-liganded [Fe-S] clusters and the nitrogen-liganded Reiske proteins suggest that the amide N and serinate O ligands to the P-cluster are both candidates as possible sites for protonation. This suggestion is further supported by the recent discovery that both of these ligands are displaced from the P-cluster upon reduction to the P^N state (*18*). Some observations from the current work provide an opportunity to explore the possible roles of these ligands in the P-cluster redox reactions. First, the results from the current work clearly point to the transfer of a single proton associated with the $P^{2+/1+}$ redox couple. This rules out the expectation for two protons associated with both the serinate-γO and amide-N ligands. In addition, the lack of a pH dependence of E_{m1} reveals that the protonatable group is no longer influencing the P^{1+} or the P^N states. Finally, because elimination of the β-Ser188 ligand by site-directed mutagenesis does not eliminate the pH dependence of E_{m2}, the serinate ligand cannot be the site of protonation. It certainly is possible that the amide ligand to the P-cluster (from Cys 88) could be undergoing protonation, although there is currently no direct evidence for this possibility. It is known that the amide ligand is displaced upon reduction of the P-cluster (*18*). Peptide amide groups typically have pK_a values of ≥13 (*52*), consistent with the pK_a^{P1+} found in the present work of >8.5 for the P^{1+} state, where the ligand is predicted not to be bound. Binding of the amide to a metal (e.g., an Fe of an Fe-S cluster) is expected to lower the pK_a (*52*), possibly to the value of 5.5 anticipated from the present work for the P^{2+} oxidation state. We are not aware of any other examples of amide ligands to [Fe-S] clusters, so there

is no precedent to guide our understanding of the properties of the amide ligand to the P-cluster. There are, however, examples of amide ligands to a mononuclear iron site in nitrile hydratase (*53*) and to model metallocenters (*52*).

There are examples from other metalloproteins that provide alternative models to explain the pH dependence of E_m for the P-cluster. For example, extensive characterization of *A. vinelandii* ferredoxin I has revealed that the E_m for the [3Fe-4S] cluster is pH dependent ($E_m = -420$, at pH 7.0) (*54*). It has been suggested that one of the inorganic sulfides of the cluster is the site of protonation. This is a reasonable possibility for the P-clusters of nitrogenase as well. Finally, it is also possible that a protonatable group near the P-cluster is imparting the pH dependence of the $P^{2+/1+}$ couple. We are currently exploring this possibility by changing amino acid residues near the P-cluster.

While the serinate ligand to the P-cluster is not the site of protonation, it is clear that this ligand does influence the electronic properties of the cluster. Removal of the serinate ligand by replacement of β-Ser188 with Gly was observed to shift both E_{m1} and E_{m2} values by over +60 mV. Previous EPR and magnetic circular dichroism studies on the thionine-oxidized β-Ser188Gly-altered MoFe protein suggested that the properties of the P-cluster were affected by the removal of the ligand (*55*). In the present work, the removal of the serinate ligand apparently changed the spin state of the P^{2+} oxidation state as evidenced by the lack of an integer spin EPR signal. The exact spin state of the P^{2+} state in the absence of a serinate ligand remains to be established. It is possible that the two cubane subclusters with $S = {}^1/_2$ are antiferromagnetically coupled resulting in an $S = 0$ spin state or ferromagnetically coupled to give an $S = 1$ spin state (*56*).

The Role of the P-Clusters in the Nitrogenase Mechanism. An obvious question about the P-clusters is why such a complex [Fe-S] cluster, with coupled electron- and proton-transfer reactions, is necessary to function as a simple electron-transfer intermediate in nitrogenase. We attempt to incorporate the current knowledge of the P-cluster into a model for the possible function in the nitrogenase reaction.

It remains difficult to explain how the P-clusters, in the P^N state, might accept electrons from the Fe protein. Indeed, it seems unlikely, and there is no direct evidence to support the further reduction of the P-clusters beyond the P^N oxidation state. This consideration suggests a different model where more oxidized states of the P-cluster function as capacitors between the Fe protein and the active-site FeMoco (*12*, *18*). In this model, the P-clusters are proposed to transfer one or more electrons to FeMoco during the catalytic cycle. The exact timing in the catalytic cycle for this reaction remains unclear, however, the results of Lowe et al. (*12*) clearly point to oxidized states of the P-cluster (probably P^{3+}) occurring during the reduction of N_2. The results from the present study demand that if the $P^{2+/1+}$ redox couple is accessed during catalysis, then the electron-transfer reaction will be coupled to a proton transfer. This is interesting considering that all substrate reduction reactions catalyzed by nitrogenase also involve proton transfer. Thus, it is tempting to speculate that the P-clusters might function in both electron and proton delivery to the active site FeMoco.

ACKNOWLEDGMENT

We thank Professors John Peters, Michael Johnson, Anthony Wedd, and Vernon Parker for helpful discussions and Jeannine Chan for critically reading this manuscript. We also thank Raymond Hellinger for technical assistance.

REFERENCES

1. Burgess, B. K., and Lowe, D. J. (1996) *Chem. Rev. 96*, 2983−3011.
2. Seefeldt, L. C., and Dean, D. R. (1997) *Acc. Chem. Res. 30*, 260−266.
3. Howard, J. B., and Rees, D. C. (1994) *Annu. Rev. Biochem. 63*, 235−264.
4. Peters, J. W., Fisher, K., and Dean, D. R. (1995) *Annu. Rev. Microbiol. 49*, 335−366.
5. Mortenson, L. E., Seefeldt, L. C., Morgan, T. V., and Bolin, J. T. (1993) *Adv. Enzymol. 67*, 299−374.
6. Hageman, R. V., and Burris, R. H. (1978) *Proc. Natl. Acad. Sci. U.S.A. 75*, 2699−2702.
7. Rasche, M. E., and Seefeldt, L. C. (1997) *Biochemistry 36*, 8574−8585.
8. McKenna, C. E., Simeonov, A. M., Eran, H., and Bravo-Leerahhandh, M. (1996) *Biochemistry 35*, 4502−4514.
9. Burgess, B. K. (1985) in *Metal Ions in Biology: Molybdenum Enzymes* (Spiro, T. G., Ed) pp 161−220, John Wiley & Sons, New York.
10. Peters, J. W., Fisher, K., Newton, W. E., and Dean, D. R. (1995) *J. Biol. Chem. 270*, 27007−27013.
11. Lanzilotta, W. N., and Seefeldt, L. C. (1996) *Biochemistry 35*, 16770−16776.
12. Lowe, D. J., Fisher, K., and Thorneley, R. N. F. (1993) *Biochem. J. 292*, 93−98.
13. Ma, L., Brosius, M. A., and Burgess, B. K. (1996) *J. Biol. Chem. 271*, 10528−10532.
14. Kim, J., and Rees, D. C. (1992) *Science 257*, 1677−1682.
15. Schindelin, H., Kisker, C., Schlessman, J. L., Howard, J. B., and Rees, D. C. (1997) *Nature 387*, 370−376.
16. Peters, J. W., Lanzilotta, W. N., Ryle, M. J., Howard, J. B., Seefeldt, L. C., and Rees, D. C. (Manuscript in preparation).
17. Johnson, M. K. (1994) in *Encyclopedia of Inorganic Chemistry* (King, R. B., Ed.) Vol. 4, pp 1896−1915, John Wiley & Sons, New York.
18. Peters, J. W., Stowell, M. H. B., Soltis, S. M., Finnegan, M. G., Johnson, M. K., and Rees, D. C. (1997) *Biochemistry 36*, 1181−1187.
19. Hurley, J. K., Weber-Main, A. M., Hodges, A. E., Stankovich, M. T., Benning, M. M., Holden, H. M., Cheng, H., Xia, B., Markley, J. L., Genzor, C., Gomez-Moreno, C., Hafezi, R., and Tollin, G. (1997) *Biochemistry 36*, 15109−15117.
20. Kowal, A. T., Werth, M. T., Manodori, A., Cecchini, G., Schroder, I., Gunsalus, R. P., and Johnson, M. K. (1995) *Biochemistry 34*, 12284−12293.
21. Augier, V., Guigliarelli, B., Asso, M., Bertrand, P., Frixon, C., Giordano, G., Chippaux, M., and Blasco, F. (1993) *Biochemistry 32*, 2013−2023.
22. Zhao, J., Li, N., Warren, P. V., Golbeck, J. H., and Bryant, D. A. (1992) *Biochemistry 31*, 5093−5099.
23. Babini, E., Bertini, I., Borsari, M., Capozzi, F., Dikiy, A., Eltis, L. D., and Luchinat, C. (1996) *J. Am. Chem. Soc. 118*, 75−80.
24. Werth, M. T., Cecchini, G., Manodori, A., Ackrell, B. A. C., Schroder, I., Gunsalus, R. P., and Johnson, M. K. (1990) *Proc. Natl. Acad. Sci. U.S.A. 87*, 8965−8969.
25. Yu, L., Bryant, D. A., and Golbeck, J. H. (1995) *Biochemistry 34*, 7861−7868.
26. Jung, Y. S., Vassiliev, I. R., Yu, J., McIntosh, L., and Golbeck, J. H. (1997) *J. Biol. Chem. 272*, 8040−8049.
27. Shen, B., Jollie, D. R., Diller, T. C., Stout, C. D., Stephens, P. J., and Burgess, B. K. (1995) *Proc. Natl. Acad. Sci. U.S.A. 92*, 10064−10068.

28. Xia, B., Cheng, H., Bandarian, V., Reed, G. H., and Markley, J. L. (1996) *Biochemistry 35*, 9488−9495.
29. Rothery, R. A., and Weiner, J. H. (1991) *Biochemistry 30*, 8296−8305.
30. Meyer, J., Gaillard, J., and Lutz, M. (1995) *Biochem. Biophys. Res. Commun. 212*, 827−833.
31. Zhou, Z. H., and Adams, M. W. W. (1997) *Biochemistry 36*, 10892−10900.
32. Seefeldt, L. C., and Mortenson, L. E. (1993) *Protein Sci. 2*, 93−102.
33. Brigle, K. E., Setterquist, R. A., Dean, D. R., Cantwell, J. S., Weiss, M. C., and Newton, W. E. (1987) *Proc. Natl. Acad. Sci. U.S.A. 84*, 7066−7069.
34. Hathaway, G. M., Lundak, T. S., Tahara, S. M., and Traugh, J. A. (1979) *Methods Enzymol. 60*, 495−511.
35. Chromy, V., Fischer, J., and Kulhanek, V. (1974) *Clin. Chem. 20*, 1362−1363.
36. Watt, G. D., and Wang, Z. C. (1989) *Biochemistry 28*, 1844−1850.
37. Seefeldt, L. C., and Ensign, S. A. (1994) *Anal. Biochem. 221*, 379−386.
38. Lanzilotta, W. N., and Seefeldt, L. C. (1997) *Biochemistry 36*, 12976−12983.
39. Ryle, M. J., and Seefeldt, L. C. (1996) *Biochemistry 35*, 4766−4775.
40. Tittsworth, R. C., and Hales, B. J. (1993) *J. Am. Chem. Soc. 115*, 9763−9767.
41. Dutton, P. L. (1978) *Methods Enzymol. 54*, 411−435.
42. Lindahl, P. A., Papaefthymiou, V., Orme-Johnson, W. H., and Münck, E. (1988) *J. Biol. Chem. 263*, 19412−19418.
43. Pierik, A. J., Wassink, H., Haaker, H., and Hagen, W. R. (1993) *Eur. J. Biochem. 212*, 51−61.
44. Lanzilotta, W. N., Fisher, K., and Seefeldt, L. C. (1996) *Biochemistry 35*, 7188−7196.
45. Zhang, H., Carrell, C. J., Huang, D., Sled, V., Ohnishi, T., Smith, J. L., and Cramer, W. A. (1996) *J. Biol. Chem. 271*, 31360−31366.
46. Fee, J. A., Findling, K. L., Yoshida, T., Hille, R., Tarr, G. E., Hearshen, D. O., Dunham, W. R., Day, E. P., Kent, T. A., and Munck, E. (1984) *J. Biol. Chem. 259*, 124−133.
47. Britt, R. D., Sauer, K., Klein, M. P., Knaff, D. B., Kriauciumas, A., Yu, C. A., Yu, L., and Malkin, R. (1991) *Biochemistry 30*, 1892−1901.
48. Link, T. A., Hagen, W. R., Pierik, A. J., Assmann, C., and Jagow, G. V. (1992) *Eur. J. Biochem. 208*, 685−691.
49. Iwasaki, T., Imai, T., Urushiyama, A., and Oshima, T. (1996) *J. Biol. Chem. 271*, 27659−27663.
50. Liebl, U., Pezennec, S., Riedel, A., Kellner, E., and Nitschke, W. (1992) *J. Biol. Chem. 267*, 14068−14072.
51. Conover, R. L., Kowal, A. T., Fu, W., Park, J. B., Aona, S., Adams, M. W. W., and Johnson, M. K. (1990) *J. Biol. Chem. 265*, 8533−8541.
52. Holm, R. H., Kennepohl, P., and Solomon, E. I. (1996) *Chem. Rev. 96*, 2239−2314.
53. Huang, W., Jia, J., Cummings, J., Nelson, M., Schneider, G., and Lindqvist, Y. (1997) *Structure 5*, 691−699.
54. Shen, B., Jollie, D. R., Stout, C. D., C., D. T., Armstrong, F. A., Gorst, C. M., La Mar, G. N., Stephens, P. J., and Burgess, B. K. (1994) *J. Biol. Chem. 269*, 8564−8575.
55. Newton, W. E., Fisher, K., Kim, C. H., Shen, J., Cantwell, J. S., Thrasher, K. S., and Dean, D. R. (1995) in *Nitrogen Fixation: Fundamentals and Applications* (Tikhonovich, I. A., Provorov, N. A., Romanov, V. I., and Newton, W. E., Eds.) pp 91−96, Kluwer Academic Publishers, Boston.
56. Mouesca, J. M., Noodleman, L., and Case, D. A. (1994) *Inorg. Chem. 33*, 4819−4830.

BI980048D